



Immobilization of aldoxime dehydratases on metal affinity resins and use of the immobilized catalysts for the synthesis of nitriles important in fragrance industry

Barbora Kříštková^{a,b}, Ludmila Martínková^{a,*}, Lenka Rucká^a, Michael Kotik^a, Natalia Kulik^c, Robert Rädisch^{a,d}, Margit Winkler^{e,f}, Miroslav Pátek^a

^a Institute of Microbiology of the Czech Academy of Sciences, Vídeňská 1083, Prague CZ-142 00, Czech Republic

^b Faculty of Food and Biochemical Technology, University of Chemistry and Technology, Prague, Technická 5, Prague CZ-166 28, Czech Republic

^c Laboratory of Photosynthesis, Centre Algatech, Institute of Microbiology of the Czech Academy of Sciences, Novohradská 237, Třeboň CZ-37981, Czech Republic

^d Department of Genetics and Microbiology, Faculty of Science, Charles University, Vinicná 5, Prague CZ-128 44, Czech Republic

^e Institute of Molecular Biotechnology, Faculty of Technical Chemistry, Chemical and Process Engineering, Biotechnology, Graz University of Technology, Petersgasse 14, Graz A-8010, Austria

^f Austrian Center of Industrial Biotechnology GmbH, Krengasse 37, Graz A-8010, Austria



ARTICLE INFO

Keywords:

Aldoxime dehydratase

Immobilization

Metal affinity resin

Phenylacetonitrile

Cinnamonnitrile

Fragrance nitriles

Chemical compounds studied in this article:

Phenylacetaldioxime (N-hydroxy-2-

phenylethanimine)

Phenylacetonitrile

E-Cinnamaldoxime (N-[(2E)-3-phenylprop-2-en-1-ylidene]hydroxylamine)

E-Cinnamonnitrile (E-3-phenylprop-2-enenitrile)

ABSTRACT

Nitriles have a wide range of uses as building blocks, solvents, and alternative fuels, but also as intermediates and components of flavors and fragrances. The enzymatic synthesis of nitriles by aldoxime dehydratase (Oxd) is an emerging process with significant advantages over conventional approaches. Here we focus on the immobilization of His-tagged Oxd on metal affinity resins, an approach that has not been used previously for these enzymes. The potential of the immobilized Oxd was demonstrated for the synthesis of phenylacetonitrile (PAN) and E-cinnamonnitrile, compounds applicable in the fragrance industry. A comparison of Talon and Ni-NTA resins showed that Ni-NTA with its higher binding capacity was more suitable for the immobilization of Oxd. Immobilized Oxd were prepared from purified enzymes (OxdFv from *Fusarium venetum* and OxdBr1 from *Baardyphizobium* sp.) or the corresponding cell-free extracts. The immobilization of cell-free extracts reduced time and cost of the catalyst production. The immobilized OxdBr1 was superior in terms of recyclability (22 cycles) in the synthesis of PAN from 15 mM E/Z-phenylacetaldioxime at pH 7.0 and 30 °C (100% conversion, 61% isolated yield after product purification). The volumetric and catalyst productivity was 10.5 g/L/h and 48.3 g/g of immobilized protein, respectively.

1. Introduction

Nitriles are of great interest as intermediates for organic synthesis and as solvents, fuels (Plass et al., 2019) or fragrances (Pei et al., 2023). A nitrile widely used as a solvent and building block is phenylacetonitrile (PAN) (Fig. 1). It can also be used as a substrate or intermediate in the production of fragrances. Its hydrolysis leads to phenylacetic acid (PAc) and can be catalyzed chemically or enzymatically (Fan et al., 2017). The reduction of PAc to 2-phenylethanol (phenethyl alcohol) can be carried out under mild conditions with sodium borohydride and iodine (Kanth and Periasamy, 1991). 2-Phenylethanol is in great demand in cosmetics and perfumery, as it is a nature-identical floral fragrance. Another fragrance compound, methyl phenylacetate

(honey fragrance), can be produced from PAN with supercritical alcohols (Hou et al., 2015). PAN is a plant defense compound that was found in the loquat tree; its biosynthesis is catalyzed by cytochrome P450 CYP77A59 in this plant (Yamaguchi et al., 2023).

E-Cinnamonnitrile (E-CinN; Fig. 1) has been used as an ingredient of room deodorants or air fresheners (<https://www.whatsinproducts.com/chemicals/view/1/5581/001885-38-7>). It has a similar odor as E-cinnamaldehyde, the natural flavor of cinnamon. Fragrance nitriles are generally more stable than the corresponding aldehydes and non-genotoxic, while their scents are similar. These are the reasons for replacing aldehyde fragrances with nitriles (Pei et al., 2023).

A conventional method for nitrile synthesis is the substitution of a leaving group (e.g., chloride) with cyanide ion (<https://pubchem.ncbi.nlm.nih.gov/compound/142>).

* Correspondence to: Institute of Microbiology of the Czech Academy of Sciences, Vídeňská-1083, Prague CZ-142 00, Czech Republic

E-mail address: martinko@biomed.cas.cz (L. Martínková).

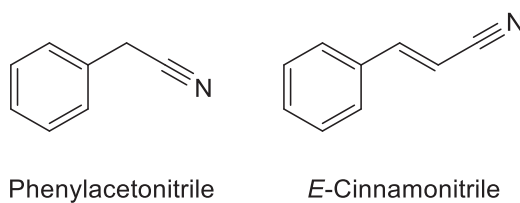


Fig. 1. Target nitriles important in fragrance industry.

[nlm.nih.gov/compound/Phenylacetonitrile#section=Methods-of-Manufacturing](https://www.ncbi.nlm.nih.gov/compound/Phenylacetonitrile#section=Methods-of-Manufacturing)). The use of highly toxic simple cyanides (KCN, NaCN) in these syntheses is a disadvantage, similar as the harsh conditions in other common methods. This is why alternative approaches are being sought (Hinzmann et al., 2020a; Pei et al., 2023).

Aldoxime dehydratase (EC 4.8.1.2.–4; Oxd) was discovered in the late 1990s and initial studies focused on its reaction mechanism and biochemical characterization. These studies were largely carried out using a core collection of Oxd from *Bacillus*, *Rhodococcus* and *Pseudomonas* (for review see Betke et al., 2018a). Later, the portfolio of Oxd was extended by, e.g., the bacterial OxdBr1 from *Bradyrhizobium* sp. (Rädisch et al., 2018) and OxdF1 from *Pseudomonas putida* (Chen et al., 2021), as well as the fungal OxdFG from *Fusarium graminearum* (Kato and Asano, 2006), OxdFv from *Fusarium vanettenii* (Kríštková et al., 2023) and OxdAsp from *Aspergillus ibericus* (Pei et al., 2023). In addition, a recent work confirmed activity in a few so far hypothetical bacterial Oxd (Hinzmann et al., 2023).

The first catalysts used for nitrile synthesis were whole cells of *Rhodococcus* sp. YH3–3 (Kato et al., 1999) or recombinant *E. coli* with the enzyme OxdB from *Bacillus* sp. OxB-1 (Xie et al., 2001), yielding various nitriles including PAN on gram scale. Further applications of Oxd for nitrile synthesis followed later and were recently reviewed (Chen, 2021; Hinzmann et al., 2021; Domínguez de María, 2021). These included the synthesis of adiponitrile on a gram scale (Betke et al., 2018b) or *n*-octanenitrile on a hundred-gram scale (Hinzmann et al., 2019b). Some studies deployed Oxd in multistep reactions with aldehydes (Zheng et al., 2022), carboxylates (Horvat et al., 2022; Winkler et al., 2023), alkenes (Plass et al., 2019), alcohols (Hinzmann et al., 2020a), or benzylamines (Xiao et al., 2023) as the starting materials. A different route from alkenes to nitriles was via dihydroisoxazoles, where Oxd catalyzed ring opening via a Kemp elimination reaction (Miao et al., 2017; Zheng and Asano, 2020).

For the above syntheses, the Oxd were largely used in the form of free whole cells, although the added value of purified enzymes are their high specific activities and the absence of side reactions catalyzed by the host enzymes. However, single use of the purified enzymes is probably uneconomical both in terms of time and cost.

Therefore, we investigated the synthesis of PAN and CinN by immobilized Oxd. The immobilization of Oxd has already attracted some attention and promising results were obtained with immobilized whole cells. For example, the cells were immobilized on a highly hydrophilic polyacrylic acid (PAA), a “superabsorber”, and proved suitable for the synthesis of *n*-octanenitrile (Hinzmann et al., 2019a), a fragrance nitrile (<https://synarome.com/compendium/octane-nitrile/>). The immobilization enabled the enzymatic conversion to be performed in pure cyclohexane (Hinzmann et al., 2019a). Entrapment of cells in calcium alginate beads coated with tetraethylorthosilicate (TEOS) also proved useful, with the enzyme OxdB performing better than OxdRE from *Rhodococcus erythropolis*. The function of TEOS was to increase the hydrophobicity of the carrier and thus its affinity to the substrate, *n*-octanaldoxime (Hinzmann et al., 2020b). The immobilization of purified Oxd was investigated with various carriers based on methacrylates or styrene but resulted in immobilized Oxd with only moderate residual activities of 5–20%. Therefore, this method was evaluated as inferior compared to immobilization of whole cells with up to 75% residual activity (Hinzmann et al., 2020b).

In this work, we were inspired by the success of the immobilization of various proteins on metal affinity resins. This type of method was introduced for the binding of His₆-tagged proteins (IL8, human tissue factor) via a nitrilotriacetic acid (NTA) derivative on microtiter plates for ligand affinity studies (Paborsky et al., 1996). Later, an analogous approach was used to prepare an immobilized GroEL for enzyme refolding (Teshima et al., 1998) and immobilized enzymes such as benzaldehyde lyase (BAL) (Kurlemann and Liese, 2004), ubiquitin C-terminal hydrolase YUH1 (Yu et al., 2007), NADH oxidase (Wang et al., 2010) or carboxylate reductase (CAR) (Maphatsoe et al., 2022).

This method is simple and selective, and usually does neither affect the enzyme activity nor interfere with the active site. In addition, the possibility of easily replacing the spent enzyme has been recognized (Kurlemann and Liese, 2004). Here, the immobilized catalysts were prepared from purified enzymes or cell-free extracts (CFEs). The latter approach, if successful, has the added advantage of eliminating the cost and time required to purify the enzyme.

2. Materials and methods

2.1. Chemicals

Talon Metal Affinity Resin (Clontech Laboratories, CA, USA) and N-NTA Agarose (Qiagen, Germany) were used for enzyme immobilization. The substrates were as described previously (Kríštková et al., 2023).

2.2. Enzyme production

Enzymes OxdFv from *F. vanettenii* 77–13–4 (protein EEU37245.1) and OxdBr1 from *Bradyrhizobium* sp. LTSPM299 (protein WP_044589203.1) were produced in *E. coli* BL21 (DE3) as described previously (Kríštková et al., 2023; Rädisch et al., 2018). The cultivation conditions were slightly changed: δ-aminolevulinic acid (Rädisch et al., 2018) was omitted from the cultivation medium.

2.3. Enzyme purification

E. coli cells were harvested and disrupted as described previously (Kríštková et al., 2023). The CFEs were used for enzyme purification or immobilization (Section 2.4.). The enzymes were purified using Talon Metal Affinity Resin as described previously (Rädisch et al., 2018; Kríštková et al., 2023) or column chromatography on a 5-mL His-Trap column (GE Healthcare). The separation conditions were as follows: binding buffer (A) – 20 mM potassium phosphate with 500 mM NaCl and 30 mM imidazole, pH 7.4; elution buffer (B) – 20 mM potassium phosphate with 500 mM NaCl and 400 mM imidazole, pH 7.4; linear gradient – 0–100% B (30 min), 2.5 mL/min. Fractions containing the enzyme were pooled and concentrated on Amicon® Ultra-15 Centrifugal Filter Units (cutoff 10 kDa, Merck Millipore). Enzyme activities were determined as described previously (Rädisch et al., 2018; Kríštková et al., 2023). The purified enzymes were used immediately or stored in phosphate buffer saline (PBS) (Kríštková et al., 2023) on ice.

2.4. Enzyme immobilization

The resin (Section 2.1.) was washed with 20 mM potassium phosphate buffer containing 10 mM imidazole and 500 mM NaCl (pH 7.4) to remove storage buffer. The volumes of resin are given without the storage buffer. The washed resin (0.13–1.0 mL) was mixed with an appropriate amount of CFE (166–240 mg protein) or 3.9–7.2 mg of purified enzyme (see Section 3.2. – 3.3. for details) and the mixture was incubated for 1 h at 4 °C. The mixture was then gently centrifuged, and the supernatant was withdrawn. The resin was washed with PBS and centrifugation was repeated. The immobilized enzymes were used immediately or stored in PBS on ice.

2.5. Reactions catalyzed by immobilized enzymes

The total volume of the reaction mixtures was 1.5 or 5 mL. (Mini) tubes with the reaction mixtures were placed in a Thermomixer Compact and shaken at 350 rpm at 30 °C. The resin with immobilized OxdFv was preincubated in Britton-Robinson buffer (Kríštková et al., 2023), pH 7.0, with additives (5.0 or 7.5 mM Na₂S₂O₄, 5.0 or 7.5 mM FeSO₄) for 10 min. The reaction was started by adding 5, 10, 15 or 20 mM E/Z-phenylacetaldoxime (E/Z-PAOx) from 100 mM, 200 mM, 300 mM, and 400 mM stock solutions in methanol, respectively. Another portion of 7.5 mM Na₂S₂O₄ and 7.5 mM FeSO₄ (total volume of 0.24 mL) was added after 10 min. After a further 10 min, the immobilized enzyme was collected by gentle centrifugation. Optionally, it was used for the next reaction under the same conditions. Samples (0.5 mL) of supernatants were supplemented with 0.1 mL of MeCN/1 M H₃PO₄ (40:60), centrifuged and analyzed by HPLC as described previously (Kríštková et al., 2023). Analogously, OxdBr1 was used for the reaction of 15 mM PAOx or 5 mM CinOx. Conversions of duplicate reactions generally varied within 5%. The concentrations of CinOx and CinN were determined by HPLC using an Ascentis® RP-Amide (250 × 4.6 mm) column and a mobile phase consisting of MeCN/water (50:50) with 0.05% H₃PO₄ at a flow rate of 1.5 mL/min and a temperature of 34 °C. In the preparative reaction of PAOx, pooled supernatants were extracted with ethyl acetate. After evaporation, the resulting crude extract was purified by silica gel column chromatography using a mobile phase consisting of ethyl acetate : cyclohexane, 5 : 95. Identity of the product PAN was determined by NMR as described previously (Rädisch et al., 2018).

2.6. Enzyme modeling and substrate docking

The templates for homology modeling of OxdBr1 were identified by BLAST search (Boratyn et al., 2012) in the protein database (Berman et al., 2000). Two conformational states – open and closed – were possible for OxdBr1. OxdRE (pdb: 3a16) from *Rhodococcus erythropolis* (Sawai et al., 2009) and OxB (pdb: 7f30) from *Bacillus* sp. (Matsui et al., 2022) were used to model the open conformation. The closed conformation was modeled using the crystal structures of the corresponding conformations of OxdRE (pdb: 3a17), OxdB (pdb: 7f2y) (Matsui et al., 2022), and OxdA (3w08) from *Pseudomonas chlororaphis* (Nomura et al., 2013). Multiple sequence alignment was built with Clustal Omega (Sievers and Higgins, 2018). It was then manually modified in Jalview (Waterhouse et al., 2009) and colored using ESPript (Robert and Gouet, 2014) (Figure S1 in Supplementary Information). Homology models were constructed with Modeller 10.3 (Šali et al., 1995) by modeling in the presence of cofactor (heme) and ligands (PAOx in 3a16, butyraldoxime in 3a17). AlphaFold has recently shown a good predictive power (Jumper et al., 2021). The models constructed by Modeller were compared with those constructed by AlphaFold downloaded from UniProt. Model refinement was performed in YASARA using a standard protocol with the Yasara2 force field in water (Land and Humble, 2018). The model was equilibrated during the first 15–30 ns of the 100-ns refinement and the structure obtained after 100 ns was used for docking. The active site residues and the oxime nitrogen atoms of the ligands were fixed during refinement. In addition, the C-alpha atoms of the helix α8 were fixed to prevent interchange between the open and closed conformation. The refined model was used for local docking using AutoDock4.2 (Morris et al., 2009) with Lamarckian genetic algorithm (Morris et al., 1998) in the presence of cofactor (heme). The structures of the ligands were built in YASARA.

3. Results

3.1. Selection of aldoxime dehydratases and substrate prediction

The enzymes used in this work (OxdFv, OxdBr1) were overproduced

and characterized in previous studies (Rädisch et al., 2018; Kríštková et al., 2023). PAOx proved to be one of the best substrates of both enzymes, which is typical for Oxd. The ferrous state of the iron cofactor is essential for Oxd function, and, therefore, oxidants can have a detrimental effect on Oxd activity. Thus, the activities of several purified Oxd were previously determined in the presence of 5 mM Na₂S₂O₄ under argon atmosphere. Under these conditions, three bacterial Oxd exhibited specific activities of 562–851 U/mg protein for Z-PAOx in contrast to OxdK from *Pseudomonas* sp. which exhibited an activity of only 2.25 U/mg (Kato and Asano, 2006). In OxdFv and OxdBr1, suitable reducing agents maintained the enzymes in their active forms under aerobic conditions. OxdFv required Fe²⁺ and Na₂S₂O₄ to support and maintain activity (Kríštková et al., 2023), while Na₂S₂O₄ was sufficient for OxdBr1 (Rädisch et al., 2018). Nevertheless, Fe²⁺ also slightly increased the activity of OxdBr1 (Figure S2 in Supplementary Information). The suitability of aerobic conditions facilitates the use of OxdFv and OxdBr1 with activities of about 25 U/mg protein (Kríštková et al., 2023) and 159 U/mg protein (Rädisch et al., 2018), respectively, for E/Z-PAOx. Nevertheless, a direct comparison of an Oxd activity under aerobic and anaerobic conditions is still lacking.

Previously, homology modeling by Modeller (Šali et al., 1995) was used to predict the affinity of OxdFv for its potential substrates (Kríštková et al., 2023). (Aryl)aliphatic aldoximes showed favorable free energies of binding in the active site of OxdFv. However, only one of the four modeled isomers of CinOx was predicted to be a good substrate for OxdFv, namely the isomer with Z-configuration and E-configuration at the C=C and C=N bonds, respectively. However, the available substrate has an E-configuration at the C=C bond. This was consistent with the experimental finding that it was a poor substrate for the purified enzyme. OxdBr1 was modeled in this work using Modeller (Šali et al., 1995) and AlphaFold. In contrast to OxdFv, the sequence of OxdBr1 shows a relatively high identity with the sequences of Oxd whose crystal structures have been determined – 46.97% with 3w08 and 3a17, and 32.63% with 7f2y. OxdBr1 belongs to the Oxd with RSH as the canonical catalytic triad in contrast to OxdFv, where the catalytic triad was suggested to be REE (Kríštková et al., 2023).

Except for catalytic residues, OxdBr1 and OxdFv differ in the β-sheet located above the bound ligand (blue dots in Figure S1) and the N-terminal part. The N-terminus of OxdBr1 has a similar length as in OxdA, whose structure has been solved, separating the active site from the bulk water and forming an entrance to the active site. In addition, OxdBr1 has a smaller serine residue at position 29 compared with Met29 found in OxdA or Phe2 at the corresponding position in OxdFv; these residues are directed inside the binding pocket (green dot on Figure S1) and can influence the size of substrates that are accepted by the enzyme.

Docking of PAOx in the model of OxdBr1 with closed conformation showed that the distance between the oxime nitrogen and the Fe²⁺ of the cofactor was smaller for Z-PAOx, although its free energy of binding was slightly higher (and the binding thus weaker) than for E-PAOx (Table 1). The model with open conformation accepted Z-PAOx but not E-PAOx. Both isomers of PAOx are present in the reaction mixtures as determined by HPLC (Kríštková et al., 2023). The binding scores indicate that CinOx has a slightly better binding affinity than PAOx (Table 1). However,

Table 1

Free energy of binding (kcal/mol) of phenylacetaldoxime (PAOx) and cinnamaldoxime (CinOx) isomers docked in the active site of OxdBr1 modeled in its closed or open conformation (see Section 2.6.).

| Conformation | Free energy of binding (kcal/mol) | | | | | |
|--------------|-----------------------------------|--------|------------------------|------------------------|------------------------|------------------------|
| | Z-PAOx | E-PAOx | E,E-CinOx ^a | Z,E-CinOx ^a | E,Z-CinOx ^a | Z,Z-CinOx ^a |
| open | -6.38 | - | -6.69 | -6.69 | - | -6.88 |
| closed | -5.98 | -6.33 | -6.84 | -6.71 | - | -6.49 |

^a The first E or Z stands for the configuration at the C=C bond. The second stands for the configuration at the C=N bond.

CinOx is more rigid, which could hinder substrate rotation (part of the catalytic cycle; Pan et al., 2012) and reduce activity. All isomers of CinOx except the isomer with *E* and *Z*-configuration at the C=C bond and C=N bond, respectively, were predicted to be substrates of OxdBr1 in both open and closed conformations. The configuration at the C=C bond is stable under the reaction conditions used. The ratio of the isomers with *E*- or *Z*-configuration at the C=N bond was not investigated during the reaction, as the two isomers were not separated by HPLC (Figure S3 in Supplementary information). However, this configuration is expected to be unstable.

3.2. Selection of carrier and enzyme source

OxdFv was used to investigate the suitability of Ni-NTA and Talon for immobilization of Oxd. Ni-NTA has a higher binding capacity of up to 50 mg of protein per mL of the resin ([https://www.qiagen.com/us/products/discovery-and-translational-research/protein-purification/detection/ni-nta-agarose](https://www.qiagen.com/us/products/discovery-and-translational-research/protein-purification/tagged-protein-expression-purification-detection/ni-nta-agarose)) than Talon with 5–15 mg of protein per mL of the resin (<https://www.takarabio.com/learning-centers/protein-research/his-tag-purification/talon-resin-selection-guide>). CFE (\approx 240 mg of protein) was applied on 1 mL of each resin. The percentage of protein bound was approximately 10% and 20% for Ni-NTA and Talon, respectively. The amount of protein bound on Talon (47 mg/mL) exceeded the binding capacity of this resin. This indicated that a considerable proportion of the protein was bound non-specifically. However, washing of the immobilized CFE with 10 mM imidazole was detrimental to the catalyst activity, and this procedure was thus rejected.

The resulting immobilized catalysts were tested with 5 mM PAOx (Fig. 2): OxdFv immobilized on Talon dehydrated PAOx with conversions of \approx 35% (average of cycles 2–6), 20%, and 13% in three successive days, whereas the conversions achieved with OxdFv immobilized on Ni-NTA were 60% (average of cycles 2–6), 60% and 13% in three successive days. The first two cycles provided a lower conversion for both catalysts. It is likely that suitable conditions have only been achieved in the third cycle. We can hypothesize that the pH or concentrations of substrate or additive(s) in the microenvironment of the enzyme were not appropriate during the first runs or that an inhibitor of the enzyme was washed out during these runs.

Purified enzyme and CFE were compared as sources of the enzyme for immobilization on Ni-NTA. Typically, the amounts of protein applied in form of CFE and the purified enzyme were 181 mg and 7.2 mg per 1.0 mL of Ni-NTA, respectively. The amount of protein bound to the resin was 44 mg and 7.2 mg, respectively. Thus, the immobilization yield was \approx 24% for CFE and \approx 100% for the purified enzyme. The former result indicates that in this case, too, there is a non-specific binding of a protein other than Oxd, as the expected content of Oxd in

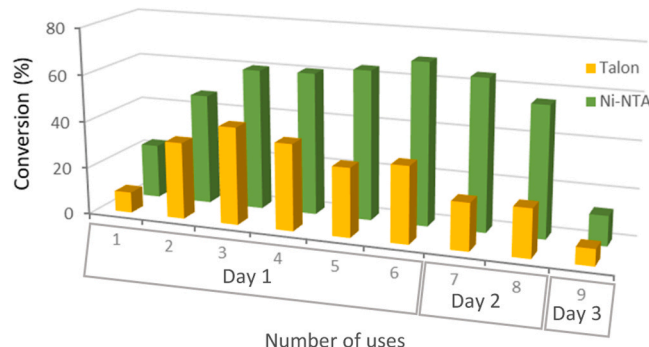


Fig. 2. Conversion of 5 mM *E/Z*-phenylacetaldoxime by aldoxime dehydratase OxdFv (cell-free extract) immobilized on Talon or Ni-NTA (1 mL of resin each; 47 mg and 24 mg of immobilized protein, respectively). Conditions: pH 7.0, 5 mM Na₂S₂O₄ and 5 mM FeSO₄, 5% MeOH, 30 °C, 10 min, 5 mL total volume. The immobilized enzymes were stored on ice between days 1, 2 and 3.

the CFE was lower (previously, 9 mg Oxd was obtained from 225 mg crude protein; Kříštková et al., 2023). Both catalysts were used for dehydration of 5 mM PAN, and their performance was comparable. Maximum conversions were achieved after two to three cycles, similar to the above experiments, and amounted to 88% for CFE and 80% for purified enzyme (Fig. 3).

3.3. Optimizing substrate conversion and catalyst recycling

We attempted to optimize the conditions to obtain a full conversion of PAOx, preferably within multiple cycles. This was achieved by adding the essential additives 7.5 mM Na₂S₂O₄ and 7.5 mM FeSO₄ in two portions in each run (Fig. 4A). The conversion of 5 mM PAOx was increased to $>$ 98% for the catalyst based on purified OxdFv. The conversion was still 97% in the fifth cycle and 92% after increasing the substrate concentration to 10 mM. About 70% conversion was achieved after increasing the concentration of PAOx to 15 mM. Analogous experiments were performed with the catalyst based on immobilized CFE, demonstrating a similar trend. Conversions from 95% to $>$ 99% were achieved in the first five cycles. After increasing the substrate concentration to 10 mM and 15 mM, the conversions were lower than for the purified enzyme, but still over 70% and around 40%, respectively. However, the conversion of 20 mM substrate was below 25% for both catalysts.

Next, recyclability of immobilized OxdFv was determined for 10 mM PAOx using fresh lots of both catalyst types (Fig. 4B). The conversion obtained for the purified enzyme was 95–98% in the first four cycles and decreased to 78% in the seventh cycle. The performance of the immobilized CFE was similar with 96% conversions in cycles 2–4 and 63% conversion in the seventh cycle.

To determine the catalyst productivity, a fresh immobilize based on purified OxdFv was used to transform 15 mM PAOx and the catalyst (3.9 mg of immobilized protein) was recycled until conversion decreased to about 50% (Fig. 5). The enzyme was thus recycled 16 times, with over 90% conversion up to cycle 11. The amount of PAN determined by HPLC was 0.328 mmol (38.4 mg), and the catalyst productivity was 9.85 mg PAN per mg of the immobilized protein.

The transformation of 15 mM PAOx was then also performed with OxdBr1 immobilized on Ni-NTA. Similar to OxdFv, the catalysts were based on the purified enzyme and CFE (Fig. 6). In the above experiments, the amount of Ni-NTA was largely in excess, especially for the purified enzyme (maximum 7.2 mg per mL of Ni-NTA) resulting in

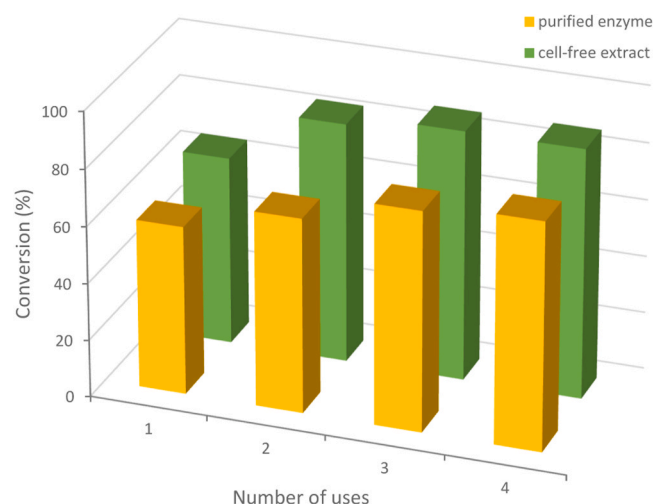


Fig. 3. Conversion of 5 mM *E/Z*-phenylacetaldoxime by aldoxime dehydratase OxdFv immobilized on Ni-NTA. The catalysts were based on purified enzyme or cell-free extract (1 mL of Ni-NTA each; 7.2 mg and 44 mg of immobilized protein, respectively). Conditions: pH 7.0, 7.5 mM Na₂S₂O₄ and 7.5 mM FeSO₄, 5% MeOH, 30 °C, 10 min, 5 mL total volume.

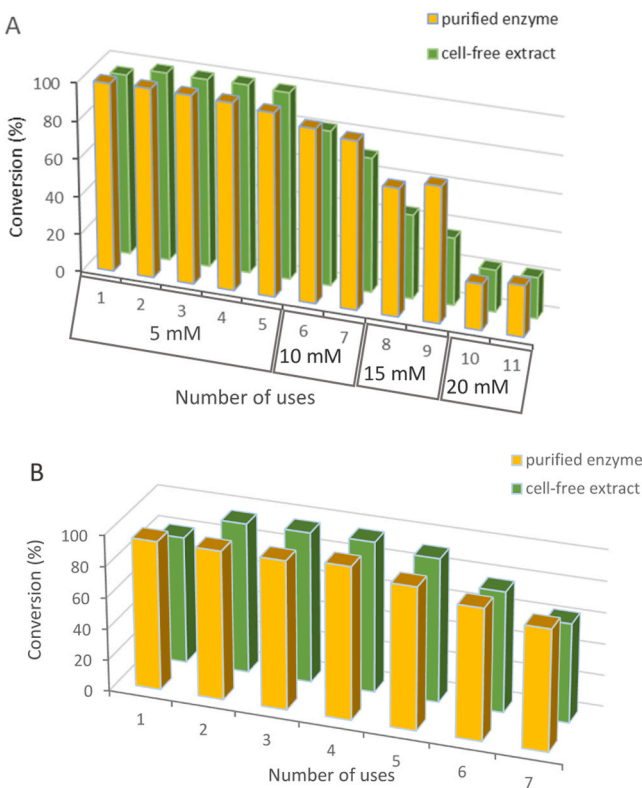


Fig. 4. Conversion of various concentrations of *E/Z*-phenylacetaldoxime by aldoxime dehydratase OxdFv immobilized on Ni-NTA. Conditions: pH 7.0, 2 × 7.5 mM Na₂S₂O₄ and 2 × 7.5 mM FeSO₄ (0 min, 10 min), 30 °C, 20 min, total volume 5 mL. (A) Substrate concentration was increased from 5 mM to 10 mM, 15 mM, and 20 mM (added from 100, 200, 300, 400 mM stock solutions of substrate in methanol) after 5, 7 and 9 cycles, respectively. All runs were performed with the same lot of catalyst based on purified enzyme (1.0 mL of Ni-NTA; 2.9 mg of immobilized protein) or CFE (0.5 mL Ni-NTA; 21 mg of immobilized protein). (B) 10 mM substrate was transformed using a fresh lot of catalyst based on purified enzyme (1.0 mL of Ni-NTA; 3.9 mg of immobilized protein) or CFE (0.5 mL Ni-NTA; 23 mg of immobilized protein), respectively.

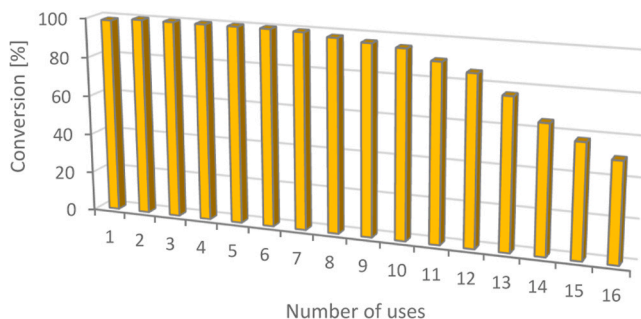


Fig. 5. Conversion of 15 mM *E/Z*-phenylacetaldoxime by purified aldoxime dehydratase OxdFv immobilized on Ni-NTA (0.13 mL; 3.9 mg of immobilized protein). Conditions: pH 7.0, 2 × 7.5 mM Na₂S₂O₄ and 2 × 7.5 mM FeSO₄ (0 min, 10 min), 30 °C, 20 min, total volume 1.5 mL.

>99% immobilization yield. Here, we reduced the amount of Ni-NTA to 0.13 mL, while the amount of purified enzyme was 3.9 mg. For unknown reasons, the amount of purified enzyme bound to the resin was 1.2 mg or 3.1 mg in two independent experiments, resulting in immobilization yields of 31% and 79%, respectively. Nevertheless, both immobilized catalysts were efficient for dehydrating PAOx and CinOx (see below). The amount of CFE applied was 166 mg protein per 0.5 mL of resin and the amount of bound protein was 27 mg or 40 mg in two

independent experiments. The immobilization yields were thus 16% and 24% for CFE.

Each of the catalysts was used 22 times without a significant decrease in PAOx conversion, which reached >99%. The amount of PAN produced by the catalyst based on purified enzyme (1.2 mg protein) was determined by HPLC to be 0.495 mmol (58.0 mg), which corresponded to a catalyst productivity of 48.3 mg PAN per mg of immobilized protein.

Reaction mixtures from two parallel reactions catalyzed by OxdBr1 (immobilized CFE) were pooled to give 116 mg of product according to HPLC. Purification of the product by flash chromatography provided ≈ 71 mg of PAN (61% isolated yield). The identity of the product was confirmed by NMR, the spectral data being the same as previously (Rädisch et al., 2018).

Previously, OxdFv was investigated for its activity toward CinOx, but OxdBr1 was not. OxdFv showed a low activity for this substrate in accordance with the results of molecular modeling (Kríštková et al., 2023). Here the ability of OxdBr1 to dehydrate CinOx was investigated with immobilized OxdBr1. The catalyst based on CFE converted >99% of CinOx to CinN (see Figure S3 for HPLC analysis), while that based on the purified OxdBr1 converted 91–95% CinOx in cycles 2–4 (Fig. 7). The activity of OxdBr1 for CinOx was consistent with the favorable docking of the substrate in the active site of the homology model (Section 3.1.). The high stability of the catalysts will probably allow for a further expansion of their reuse in PAN and CinN synthesis.

4. Discussion

In this study, we investigated the activities and stabilities of new Oxd catalysts based on immobilizing cell-free preparations (crude or purified enzymes) on metal affinity resins. To our knowledge, this type of immobilization has not yet been used for Oxd catalysts. Moreover, the (partly) purified enzymes have rarely been used for nitrile synthesis, not even in their soluble form. Although whole-cell Oxd catalysts can be very efficient, alternative solutions are worth investigating. The use of (semi-)purified enzymes could reduce the contamination of reaction mixtures with cell components including unwanted enzymes that may lead to byproducts, and thus simplify the separation of the product. Compared to recombinant cells, this may also reduce variability between catalyst batches. However, soluble enzymes can complicate the extraction of products with organic solvents by forming precipitates (Hinzmann et al., 2020b). Immobilization promises to keep the advantages of free purified enzymes while eliminating their disadvantages. In addition, immobilization of enzymes can offer known benefits such as increasing catalyst productivity and enabling process performance in continuous mode (Meyer et al., 2022).

Anaerobic conditions were reported for a superior performance of Oxd (Kato and Asano, 2006), which could discourage researchers from using purified Oxd in synthesis. Nevertheless, purified OxdFv and OxdBr1 showed satisfactory activities under aerobic conditions (Rädisch et al., 2018; Kríštková et al., 2023). These enzymes were used in the present study and their immobilization on metal affinity resin resulted in highly active catalysts. Hence, a proof-of-concept has been provided for the synthesis of PAN and CinN.

The precursor of PAN, PAOx, is a good substrate for Oxd from several bacteria and fungi, as shown by the specific and relative activities, as well as the kinetic parameters (Betke et al., 2018a; Rädisch et al., 2018; Kríštková et al., 2023). The synthesis of PAN and other nitriles was demonstrated with whole cells of recombinant *E. coli* that produced the enzyme OxdB from *Bacillus* sp. OxB-1. In addition to PAN, the nitriles prepared with this catalyst were 3-phenylpropionitrile, *n*-butyronitrile, *n*-valeronitrile and *n*-capronitrile, whereby the reactions were carried out on a gram scale (Xie et al., 2001). The substrate concentrations were considerable (100–750 mM). For example, 5.2 g of PAN (purified by distillation) was obtained from 500 mM Z-PAOx with 89% isolated yield. The time required to complete the reaction was 8 hours, which

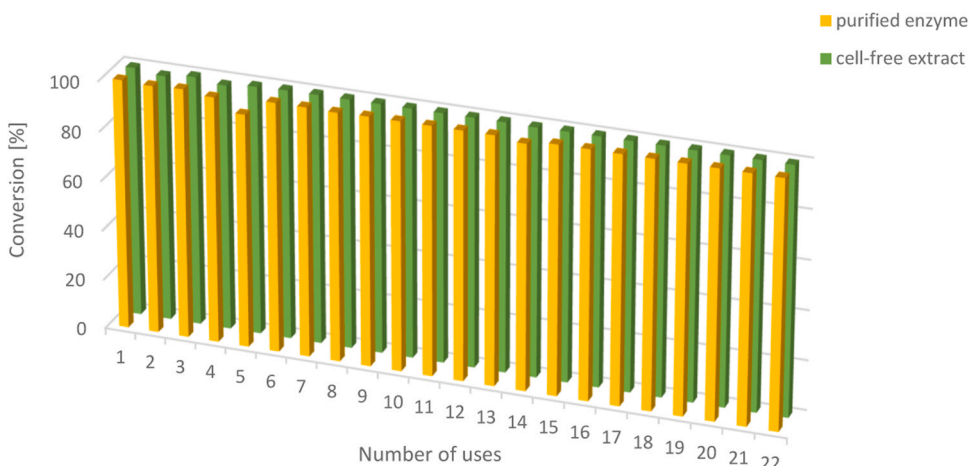


Fig. 6. Conversion of 15 mM *E/Z*-phenylacetaldoxime by aldoxime dehydratase OxdBr1 immobilized on Ni-NTA. Conditions: pH 7.0, 7.5 mM Na₂S₂O₄, 7.5 mM FeSO₄, 30 °C, 10 min, 5% MeOH, 1.5 mL total volume. The catalyst was based on purified enzyme (0.13 mL of Ni-NTA; 1.2 mg of immobilized protein) or cell-free extract (0.5 mL of Ni-NTA; 27 mg of immobilized protein).

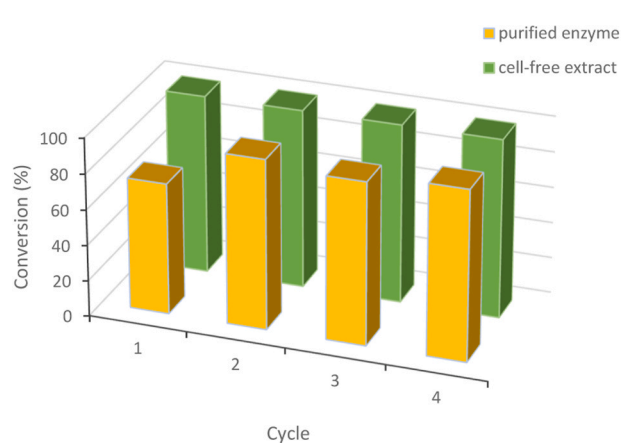


Fig. 7. Conversion of 5 mM *E/Z*-cinnamaldoxime by aldoxime dehydratase OxdBr1 immobilized on Ni-NTA. Conditions: pH 7.0, 7.5 mM Na₂S₂O₄, 7.5 mM FeSO₄, 30 °C, 20 min, 5% MeOH, 1.5 mL total volume. The catalyst was based on purified enzyme (0.13 mL of Ni-NTA; 3.1 mg of immobilized protein) or cell-free extract (0.5 mL of Ni-NTA; 40 mg of immobilized protein).

resulted in a volumetric productivity of 6.5 g/L/h. The catalyst productivity was 2.81 g/g wet cells. At a ratio of wet mass to dry mass of about 5:1 and a ratio of dry mass to protein of about 2:1, the catalyst productivity is ≈ 14 g/g dry cells and ≈ 28 g/g protein. The relatively low solubility of PAOx in water is probably a limiting factor for its biotransformation. In another approach, lower concentrations of PAN were produced by *E. coli* cultures producing cytochrome CYP79A2 from *Arabidopsis thaliana* and OxdB. The substrate L-Phe (4.1 mM) was added in the form of casamino acid nutrient (2%), and the conversion to PAN (2.75 mM) was 67% after 54 hours (Miki and Asano, 2014). The volumetric productivity was thus rather low at about 0.006 g/L/h. Supplementing the medium with 20 mM L-Phe increased PAN concentration to 4.87 mM and the volumetric productivity to 0.011 g/L/h.

Purified Oxd from *Bacillus* sp. OxB-1 (Kato et al., 2000) and OxdFv from *Fusarium vanettenii* (Kříšková et al., 2023) were used for PAN production at analytical scale. The concentration of PAOx was relatively low, but the short reaction time was advantageous. For example, OxdFv (0.19 U per 0.5 mL, i.e. ≈ 15 mg/L) converted 80% of 5 mM *E/Z*-PAOx to PAN within ≈ 30 min, and OxdB (1.0 U per 0.5 mL, i.e. ≈ 234 mg/L) converted 100% of 5 mM Z-PAOx to PAN within ≈ 15 min (Kato et al., 2000). The volumetric productivities were thus ≈ 0.94 g/L/h and ≈ 2.3 g/L/h, while the catalyst productivities were ≈ 31 g and ≈ 2.5 g of

PAN/g protein, respectively. Purified OxdBr1 (12.4 mg/L) was used to synthesize PAN (5 mM) at preparative scale (50 mL) (Rädisch et al., 2018). The product (0.188 mmol, 22 mg) was obtained after a 60-min reaction with an isolated yield of 75%, resulting in a volumetric productivity of 0.44 g/L/h and a catalyst productivity of 35.5 g/g of protein. When immobilized Oxd were used in this study, the volumetric productivity was higher than those shown above, namely 10.5 g/L/h. The maximum catalyst productivity achieved here (48.3 g/g of immobilized OxdBr1) was also the highest. However, it was only about 36% higher than that calculated for the single use of OxdBr1 (35.5 g/g protein). This was probably caused by the very high protein loading of the immobilizate. However, this high loading is likely to compensate for the loss of specific activity during the use of the catalyst. The ratio between the productivities of the immobilized and soluble enzymes is likely to increase if the immobilizate is recycled more times, which seems to be feasible with immobilized OxdBr1.

The precursor of CinN, cinnamaldoxime (CinOx), is less prone to dehydration by Oxd than PAOx. For example, the relative activity of purified OxdK from *Pseudomonas* sp. was 17% compared to PAOx (Kato and Asano, 2006), i.e. ≈ 0.38 U/mg protein. A similar activity may be expected for OxdA, as, according to YASARA, the residues within 5 Å from a substrate are the same in both enzymes. Recently, the new OxdAsp from *A. ibericus* exhibited an activity of almost 1.0 U/mg protein for CinOx (Pei et al., 2023). In addition, whole cells of *E. coli* carrying OxdAsp dehydrated 100 mM CinOx to CinN at an almost quantitative conversion. Two doses of the catalyst (33 mg wet weight per mL) were required to achieve this conversion within 5 h. The volumetric productivity and catalyst productivity were thus 2.58 g/L/h and 2.17 g/g wet cells (10.85 g/dry cells, 21.7 g/g protein). Here, we demonstrated a virtually full enzymatic conversion of CinOx to CinN by an immobilizate based on CFE, while the conversion was 91–95% for an immobilizate based on purified OxdBr1 in cycles 2–4. The higher volumetric productivity of 1.94 g/L/h was obtained for the former, and the higher catalytic productivity of 1.10 g/g protein was obtained for the latter. They can probably be increased by further recycling of the catalyst and by exploring other conditions such as the ratio of substrate to catalyst loading.

OxdBr1 appears to be one of the best Oxd due to its high specific activity and the fact that no special reaction conditions such as an inert atmosphere are required. Whereas OxdFv is attractive from an academic point of view as it is an atypical Oxd, OxdBr1 seems to be one of the workhorses among the Oxd. OxdBr1 was recently used in combination with the CAR from *Neurospora crassa* to produce PAN (≈ 0.87 g) from PAc (1.3 g) in a multistep reaction (Winkler et al., 2023).

Immobilization of OxdBr1 will undoubtedly increase its utility for nitrile synthesis including cascade reactions, but the enzyme load and the reaction conditions require further optimization to make maximum use of the enzyme. The future tasks will also involve determining the potential and limitations of the enzyme in terms of substrate range and scale-up.

Thus, immobilized OxdFv and OxdBr1 were found to be suitable for the conversion of some aldoximes to nitriles, in contrast to the previous immobilizes based on purified enzymes. Those catalysts including OxdB or OxdRE immobilized on hydrophobic, amino or epoxy resins were excluded from further investigations due to their low residual activities compared to soluble enzymes. In addition, these immobilizes were largely unstable during short-term (1 h) storage at 30 °C or long-term (32 days) storage at 4 °C (Hinzmann et al., 2020b). Thus, the catalysts presented in our work appear to be the first fully functional immobilized Oxd based on cell-free preparations. Prior to our work, the only Oxd immobilizes that showed promise for nitrile synthesis were whole cells immobilized in either PAA (for organic media) or calcium alginate (for aqueous media). However, reuse of more than three times led to a significant decrease in activity of the Si-coated alginate beads. The maximum conversion that can be achieved with this catalyst was not tested. This was only reported for OxB immobilized in PAA. A flow reactor packed with this immobilize (1 mL, 66 mg of wet cells) exhibited a stable conversion of over 95% of 0.1 M *n*-octanaldoxime within 3 hours (Hinzmann et al., 2019a). Thus, the PAA-immobilized whole cells (Hinzmann et al., 2019a) and the Ni-NTA-immobilized enzymes (this work) were the only Oxd for which the benefits of immobilization (continuous use or reusability) were clearly demonstrated.

Despite recent achievements in Oxd catalysis, transferring the process to industry is a challenge. Substrate concentration is generally a key factor for industrial viability of the process. For Oxd, considerable substrate concentrations (0.1 M to 1.0 M) were used in the reactions catalyzed by non-immobilized cells. The substrates were several aliphatic aldoximes with 6–12 carbon atoms. The low solubility of the substrates in aqueous media is problematic, but was addressed by adding the substrate in portions, resulting in a total substrate load of 4.65 M in *n*-octanaldoxime (Hinzmann et al., 2019b). This means that the whole-cell catalyzed processes have a high degree of technological maturity.

An almost complete conversion at the above substrate concentrations required the use of 33 g wet cells per L of the reaction mixture, i.e. cells from about 1.7 L of the culture (Hinzmann et al., 2019b). This seems to be acceptable in terms of the required culture size. Nevertheless, the scale-up of the culture must be addressed. This can be complicated because of the need for specific aeration conditions, which can be influenced, e.g., by the ratio of the culture vessel and medium volume (Kato and Asano, 2006).

There is still a lack of data that would allow us to evaluate the potential of immobilized catalysts for the transformation of high substrate concentrations required for mature technologies. Therefore, the immobilized enzymes obtained in this work must be tested under industrially relevant conditions. In addition, the advantages of the immobilized enzymes (recyclability, flow mode) still need to be carefully weighed against the costs of the additional operations.

5. Conclusion

The purified OxdFv and OxdBr1 and the corresponding CFEs were immobilized on Ni-NTA, which resulted in functional and reusable catalysts. The activity and recyclability were found to be similar for both types of catalysts based on either CFEs or the purified enzymes. Hence, we concluded that purification of the enzymes is not necessary because enrichment and immobilization of Oxd can be performed in a single step. The percentage of CFE protein retained on the resin suggests that the immobilized catalyst contains some non-specifically bound proteins, which could potentially result in unwanted reactions. However, no such reactions were observed in our case. The results obtained - in particular

for OxdBr1- suggest that CFE-based immobilized enzyme could be used in the future for the synthesis of PAN, CinN and possibly other nitriles from aldoximes or other starting materials such as carboxylic acids.

CRediT authorship contribution statement

Miroslav Pátek: Writing – review & editing, Project administration, Funding acquisition. **Margit Winkler:** Writing – review & editing, Project administration, Funding acquisition, Conceptualization. **Robert Rädisch:** Methodology, Investigation. **Natalia Kulik:** Writing – original draft, Methodology, Investigation, Conceptualization. **Ludmila Martínková:** Writing – review & editing, Writing – original draft, Supervision, Conceptualization. **Barbora Kríštková:** Writing – review & editing, Methodology, Investigation. **Michael Kotik:** Writing – review & editing, Methodology, Investigation. **Lenka Rucká:** Methodology, Investigation.

Declaration of Competing Interest

Coauthor Dr. Margit Winkler is Associate Editor of Journal of Biotechnology.

Data availability

Data will be made available on request.

Acknowledgement

This work was supported by the Czech Science Foundation [grant number GF20-23532 L], the Austrian Science Fund FWF [grant number I 4607], the Ministry of Education, Youth and Sports of the Czech Republic grant Talking microbes - understanding microbial interactions within One Health framework [CZ.02.01.01/00/22_008/0004597], and Czech Academy of Sciences [grant number RVO61388971]. The authors thank Dr. Helena Pelantová (Institute of Microbiology) for NMR measurement and Mr. Pavel Vávra (Institute of Microbiology) for product purification.

Appendix A. Supporting information

Supplementary data associated with this article can be found in the online version at doi:10.1016/j.biotec.2024.02.005.

References

- Berman, H.M., Westbrook, J., Feng, Z., Gilliland, G., Bhat, T.N., Weissig, H., Shindyalov, I.N., Bourne, P.E., 2000. The protein data bank. *Nucleic Acids Res* 28, 235–242. <https://doi.org/10.1093/nar/28.1.235>.
- Betke, T., Higuchi, J., Rommelmann, P., Oike, K., Nomura, T., Kato, Y., Asano, Y., Gröger, H., 2018a. Biocatalytic synthesis of nitriles through dehydration of aldoximes: the substrate scope of aldoxime dehydratases. *Chembiochem* 19, 768–779. <https://doi.org/10.1002/cbic.201700571>.
- Betke, T., Maier, M., Gruber-Wölfler, H., Gröger, H., 2018b. Biocatalytic production of adiponitrile and related aliphatic linear alpha,omega-dinitriles. *Nat. Commun.* 9, 5112. <https://doi.org/10.1038/s41467-018-07434-0>.
- Boratyn, G.M., Schäffer, A.A., Agarwala, R., Altschul, S.F., Lipman, D.J., Madden, T.L., 2012. Domain enhanced lookup time accelerated BLAST. *Biol. Direct* 7, 12. <https://doi.org/10.1186/1745-6150-7-12>.
- Chen, K., 2021. Recent progress on discovery and research of aldoxime dehydratases. *Green Synth. Catal.* 2, 179–186. <https://doi.org/10.1016/j.gresc.2021.04.001>.
- Chen, Z.J., Mao, F.Y., Zheng, H.T., Xiao, Q.J., Ding, Z.H., Wang, A.M., Pei, X.L., 2021. Cyanide-free synthesis of aromatic nitriles from aldoximes: discovery and application of a novel heme-containing aldoxime dehydratase. *Enzyme Microb. Technol.* 150, 109883 <https://doi.org/10.1016/j.enzmictec.2021.109883>.
- Domínguez de María, P., 2021. Nitrile synthesis with aldoxime dehydratases: a biocatalytic platform with applications in asymmetric synthesis, bulk chemicals, and biorefineries. *Molecules* 26, 4466. <https://doi.org/10.3390/molecules26154466>.
- Fan, H., Chen, L., Sun, H., Wang, H., Liu, Q., Ren, Y., Wei, D., 2017. Development of nitrilase-mediated process for phenylacetic acid production from phenylacetone nitrile. *Chem. Pap.* 71, 1985–1992. <https://doi.org/10.1007/s11696-017-0192-x>.
- Hinzmann, A., Adebar, N., Betke, T., Leppin, M., Gröger, H., 2019a. Biotransformations in pure organic medium: organic solvent-labile enzymes in the batch and flow

- synthesis of nitriles. *Eur. J. Org. Chem.* 2019, 6911–6916. <https://doi.org/10.1002/ejoc.201901168>.
- Hinzmann, A., Betke, T., Asano, Y., Gröger, H., 2021. Synthetic processes toward nitriles without the use of cyanide: a biocatalytic concept based on dehydration of aldoximes in water. *Chem.-Eur. J.* 27, 5313–5321. <https://doi.org/10.1002/chem.202001647>.
- Hinzmann, A., Glinski, S., Worm, M., Gröger, H., 2019b. Enzymatic synthesis of aliphatic nitriles at a substrate loading of up to 1.4 kg/l: a biocatalytic record achieved with a heme protein. *J. Org. Chem.* 84, 4867–4872. <https://doi.org/10.1021/acs.joc.9b00184>.
- Hinzmann, A., Stricker, M., Gröger, H., 2020a. Chemoenzymatic cascades toward aliphatic nitriles starting from biorenewable feedstocks. *ACS Sustain. Chem. Eng.* 8, 17088–17096. <https://doi.org/10.1021/acssuschemeng.0c04981>.
- Hinzmann, A., Stricker, M., Gröger, H., 2020b. Immobilization of aldoxime dehydratases and their use as biocatalysts in aqueous reaction media. *Catalysts* 10, 1073. <https://doi.org/10.3390/catal10091073>.
- Hinzmann, M., Yavuzer, H., Hinzmann, A., Gröger, H., 2023. Database-driven in silico-identification and characterization of novel aldoxime dehydratases. *J. Biotechnol.* 367, 81–88. <https://doi.org/10.1016/j.jbiotec.2023.02.007>.
- Horvat, M., Weilch, V., Rädisch, R., Hecko, S., Schiefer, A., Rudroff, F., Wilding, B., Klempier, N., Pátek, M., Martínková, L., Winkler, M., 2022. Chemoenzymatic one-pot reaction from carboxylic acid to nitrile via oxime. *Catal. Sci. Technol.* 12, 62–66. <https://doi.org/10.1039/d1cy01694f>.
- Hou, Z.Q., Zhang, R.Z., Luo, L.G., Yang, J., Liu, C.Z., Wang, Y.Y., Dai, L.Y., 2015. Conversion of phenylacetonitrile in supercritical alcohols within a system containing small volume of water. *Chem. Pap.* 59, 490–494. <https://doi.org/10.1515/chemapp-2015-0047>.
- Juniper, J., Evans, R., Pritzel, A., Green, T., Figurnov, M., Ronneberger, O., Tunyasuvunakool, K., Bates, R., Zídek, A., Potapenko, A., Bridgland, A., Meyer, C., Kohl, S.A.A., Ballard, A.J., Cowie, A., Romera-Paredes, B., Nikолов, S., Jain, R., Adler, J., Back, T., Petersen, S., Reiman, D., Clancy, E., Zielinski, M., Steinegger, M., Pacholska, M., Berghammer, T., Bodenstein, S., Silver, D., Vinyals, O., Senior, A.W., Kavukcuoglu, K., Kohli, P., Hassabis, D., 2021. Highly accurate protein structure prediction with AlphaFold. *Nature* 596, 583. <https://doi.org/10.1038/s41586-021-03819-2>.
- Kanth, J.V.B., Periasamy, M., 1991. Selective reduction of carboxylic-acids into alcohols using NaBH₄ and I₂. *J. Org. Chem.* 56, 5964–5965. <https://doi.org/10.1021/jo00020a052>.
- Kato, Y., Asano, Y., 2006. Molecular and enzymatic analysis of the "aldoxime-nitrile pathway" in the glutaronitrile degrader *Pseudomonas* sp. K-9. *Appl. Microbiol. Biotechnol.* 70, 92–101.
- Kato, Y., Nakamura, K., Sakiyama, H., Mayhew, S.G., Asano, Y., 2000. Novel heme-containing lyase, phenylacetaldoxime dehydratase from *Bacillus* sp. strain OxB-1: purification, characterization, and molecular cloning of the gene. *Biochemistry* 39, 800–809. <https://doi.org/10.1007/s00253-005-0044-4>.
- Kato, Y., Ooi, R., Asano, Y., 1999. A new enzymatic method of nitrile synthesis by *Rhodococcus* sp. strain YH3-3. *J. Mol. Catal. B: Enzym.* 6, 249–256. [https://doi.org/10.1016/S1381-1177\(98\)00080-0](https://doi.org/10.1016/S1381-1177(98)00080-0).
- Kríštková, B., Rädisch, R., Kulik, N., Horvat, M., Rucká, L., Grulich, M., Rudroff, F., Kádeck, A., Pátek, M., Winkler, M., Martínková, L., 2023. Scanning aldoxime dehydratase sequence space and characterization of a new aldoxime dehydratase from *Fusarium venetenii*. *Enzyme Microb. Technol.* 164, 110187. <https://doi.org/10.1016/j.enzmictec.2022.110187>.
- Kurleemann, N., Liese, A., 2004. Immobilization of benzaldehyde lyase and its application as a heterogeneous catalyst in the continuous synthesis of a chiral 2-hydroxy ketone. *Tetrahedron-Asymmetry* 15, 2955–2958. <https://doi.org/10.1016/j.tetasy.2004.07.039>.
- Land, H., Humble, M.S., 2018. YASARA: A tool to obtain structural guidance in biocatalytic investigations. In: Bornscheuer, U.T., Höhne, M. (Eds.), Protein Engineering: Methods and Protocols. Humana, New York, NY, pp. 43–67. https://doi.org/10.1007/978-1-4939-7366-8_4.
- Maphatsoe, M.M., Hashem, C., Ling, J.G., Horvat, M., Rumbold, K., Abu Bakar, F.D., Winkler, M., 2022. Characterization and immobilization of *Pycnoporus cinnabarinus* carboxylic acid reductase, PCAR2. *J. Biotechnol.* 345, 47–54. <https://doi.org/10.1016/j.jbiotec.2021.12.010>.
- Matsui, D., Muraki, N., Chen, K., Mori, T., Ingram, A.A., Oike, K., Gröger, H., Aono, S., Asano, Y., 2022. Crystal structural analysis of aldoxime dehydratase from *Bacillus* sp. OXB-1: importance of surface residues in optimization for crystallization. *J. Inorg. Biochem.* 230, 111770. <https://doi.org/10.1016/j.jinorgbio.2022.111770>.
- Meyer, L.-E., Hobisch, M., Kara, S., 2022. Process intensification in continuous flow biocatalysis by up and downstream processing strategies. *Curr. Opin. Biotechnol.* 78, 102835. <https://doi.org/10.1016/j.copbio.2022.102835>.
- Miao, Y., Metzner, R., Asano, Y., 2017. Kemp elimination catalyzed by naturally occurring aldoxime dehydratases. *ChemBioChem* 18, 451–454. <https://doi.org/10.1002/cbic.201600596>.
- Miki, Y., Asano, Y., 2014. Biosynthetic pathway for the cyanide-free production of phenylacetonitrile in *Escherichia coli* by utilizing plant cytochrome P450 79A2 and bacterial aldoxime dehydratase. *Appl. Environ. Microbiol.* 80, 6828–6836. <https://doi.org/10.1128/aem.01623-14>.
- Morris, G.M., Goodsell, D.S., Halliday, R.S., Huey, R., Hart, W.E., Belew, R.K., Olson, A.J., 1998. Automated docking using a Lamarckian genetic algorithm and an empirical binding free energy function. *J. Comput. Chem.* 19, 1639–1662. doi:10.1002/(sici)1096-987x(19981115)19:14<1639::aid-jcc10>3.0.co;2-b.
- Morris, G.M., Huey, R., Lindstrom, W., Sanner, M.F., Belew, R.K., Goodsell, D.S., Olson, A.J., 2009. AutoDock4 and AutoDockTools4: automated docking with selective receptor flexibility. *J. Comput. Chem.* 30, 2785–2791. <https://doi.org/10.1002/jcc.21256>.
- Nomura, J., Hashimoto, H., Ohta, T., Hashimoto, Y., Wada, K., Naruta, Y., Oinuma, K., Kobayashi, M., 2013. Crystal structure of aldoxime dehydratase and its catalytic mechanism involved in carbon–nitrogen triple-bond synthesis. *Proc. Natl. Acad. Sci. USA* 110, 2810–2815. <https://doi.org/10.1073/pnas.1200338110>.
- Paborosky, L.R., Dunn, K.E., Gibbs, C.S., Dougherty, J.P., 1996. A nickel chelate microtitre plate assay for six histidine-containing proteins. *Anal. Biochem.* 234, 60–65. <https://doi.org/10.1006/abio.1996.0050>.
- Pan, X.-L., Cui, F.-C., Liu, W., Liu, J.-Y., 2012. QM/MM study on the catalytic mechanism of heme-containing aliphatic aldoxime dehydratase. *J. Phys. Chem. B* 116, 5689–5693. <https://doi.org/10.1021/jp302114d>.
- Pei, X., Xiao, Q., Feng, Y., Chen, L., Yang, F., Wang, Q., Li, N., Wang, A., 2023. Enzymatic properties of a non-classical aldoxime dehydratase capable of producing alkyl and arylalkyl nitriles. *Appl. Microbiol. Biotechnol.* 107, 7089–7104. <https://doi.org/10.1007/s00253-023-12767-y>.
- Plass, C., Hinzmann, A., Terhors, M., Brauer, W., Oike, K., Yavuzer, H., Asano, Y., Vorholt, A.J., Berke, T., Gröger, H., 2019. Approaching bulk chemical nitriles from alkenes: a hydrogen cyanide-free approach through a combination of hydroformylation and biocatalysis. *ACS Catal.* 9, 5198–5203. <https://doi.org/10.1021/acscatal.8b05062>.
- Rädisch, R., Chmátl, M., Rucká, L., Novotný, P., Petrášková, L., Halada, P., Kotik, M., Pátek, M., Martínková, L., 2018. Overproduction and characterization of the first enzyme of a new aldoxime dehydratase family in *Bradyrhizobium* sp. *Int. J. Biol. Macromol.* 115, 746–753. <https://doi.org/10.1016/j.ijbiomac.2018.04.103>.
- Robert, X., Gouet, P., 2014. Deciphering key features in protein structures with the new ENDSCRIPT server. *Nucleic Acids Res.* 42, W320–W324. <https://doi.org/10.1093/nar/gku316>.
- Sali, A., Potterton, L., Yuan, F., van Vlijmen, H., Karplus, M., 1995. Evaluation of comparative protein modeling by MODELLER. *Proteins* 23, 318–326. <https://doi.org/10.1002/prot.340230306>.
- Sawai, H., Sugimoto, H., Kato, Y., Asano, Y., Shiro, Y., Aono, S., 2009. X-ray crystal structure of Michaelis complex of aldoxime dehydratase. *J. Biol. Chem.* 284, 32089–32096. <https://doi.org/10.1074/jbc.M109.018762>.
- Sievers, F., Higgins, D.G., 2018. Clustal Omega for making accurate alignments of many protein sequences. *Protein Sci.* 27, 135–145. <https://doi.org/10.1002/pro.3290>.
- Teshima, T., Mashimo, S., Kondo, A., Fukuda, H., 1998. Affinity purification and immobilization of fusion chaperonin GroEL(His)₆ and its utilization to mediate protein refolding. *J. Ferment. Bioeng.* 86, 357–362. [https://doi.org/10.1016/s0922-338x\(99\)89004-7](https://doi.org/10.1016/s0922-338x(99)89004-7).
- Wang, L., Wei, L., Chen, Y., Jiang, R., 2010. Specific and reversible immobilization of NADH oxidase on functionalized carbon nanotubes. *J. Biotechnol.* 150, 57–63. <https://doi.org/10.1016/j.jbiotec.2010.07.005>.
- Waterhouse, A.M., Procter, J.B., Martin, D.M.A., Clamp, M., Barton, G.J., 2009. Jalview Version 2-a multiple sequence alignment editor and analysis workbench. *Bioinformatics* 25, 1189–1191. <https://doi.org/10.1093/bioinformatics/btp033>.
- Winkler, M., Horvat, M., Schiefer, A., Weilch, V., Rudroff, F., Pátek, M., Martínková, L., 2023. Organic acid to nitrile: a chemoenzymatic three-step route. *Adv. Synth. Catal.* 365, 37–42. <https://doi.org/10.1002/adsc.202201053>.
- Xiao, Q.J., Feng, Y.M., Chen, L., Li, M., Zhang, P.F., Wang, Q.Y., Wang, A.M., Pei, X.L., 2023. Engineered aldoxime dehydratase to enable the chemoenzymatic conversion of benzyl amines to aromatic nitriles. *Bioorg. Chem.* 134 <https://doi.org/10.1016/j.bioorg.2023.106468>.
- Xie, S.X., Kato, Y., Asano, Y., 2001. High yield synthesis of nitriles by a new enzyme, phenylacetaldoxime dehydratase, from *Bacillus* sp. strain OXB-1. *Biosci. Biotechnol. Biochem.* 65, 2666–2672. <https://doi.org/10.1271/bbb.65.2666>.
- Yamaguchi, T., Nomura, T., Asano, Y., 2023. Identification and characterization of cytochrome P450 CYP77A59 of loquat (*Rhaphiolepis bibas*) responsible for biosynthesis of phenylacetonitrile, a floral nitrile compound. *Planta* 257, 114. <https://doi.org/10.1007/s00425-023-04151-x>.
- Yu, H.A., Kim, S.G., Kim, E.J., Lee, W.J., Kim, D.O., Park, K., Park, Y.C., Seo, J.H., 2007. Characterization of ubiquitin C-terminal hydrolase 1 (YUH1) from *Saccharomyces cerevisiae* expressed in recombinant *Escherichia coli*. *Protein Expr. Purif.* 56, 20–26. <https://doi.org/10.1016/j.pep.2007.07.005>.
- Zheng, D., Asano, Y., 2020. Biocatalytic asymmetric ring-opening of dihydroisoazoles: a cyanide-free route to complementary enantiomers of β-hydroxy nitriles from olefins. *Green. Chem.* 22, 4930–4936. <https://doi.org/10.1039/d0gc01445a>.
- Zheng, H.T., Xiao, Q.J., Mao, F.Y., Wang, A.M., Li, M., Wang, Q.Y., Zhang, P.F., Pei, X.L., 2022. Programing a cyanide-free transformation of aldehydes to nitriles and one-pot synthesis of amides through tandem chemo-enzymatic cascades. *RSC Adv.* 12, 17873–17881. <https://doi.org/10.1039/d2ra03256b>.